Associating-polymer effects in a Hele-Shaw experiment

H. Zhao and J. V. Maher
Department of Physics and Astronomy, University of Pittsburgh, Pittsburgh, Pennsylvania 15260
(Received 15 September 1992; revised manuscript received 18 February 1993)

Pattern formation is studied by injecting water into a radial Hele-Shaw cell filled with an aqueous solution of hydrophobically terminated polyoxyethylene, which forms a reversible associating network in water. A crossover from fingering pattern to fracturing pattern is demonstrated as the injection rate exceeds a threshold value. The fingering-fracturing transition is sufficiently abrupt that no gradual crossover has been observed within our limits of experimental control, and it is found to be consistent with a Deborah-number scaling, except for homopolymers (where the hydrophobic end caps are replaced by hydroxyl groups) for which the fingering-fracturing transition was never observed.

PACS number(s): 47.50.+d, 47.20.−k, 46.30.Nz

Pattern formation in nonequilibrium growth systems has attracted great attention in the past decade. The simplest of the many pattern-forming systems is a fluid-fluid displacement in a Hele-Shaw cell wherein a less viscous fluid invades a more viscous one [1, 2]. The viscous-fingering (VF) pattern formed at the unstable interface provides a rich subject for nonlinear dynamics study. The Hele-Shaw VF problem for simple Newtonian fluids is reasonably well understood now, whereas for non-Newtonian fluids our understanding is far from complete. Earlier work of Nittman, Daccord, and Stanley [3, 4] has shown that the patterns become much more ramified, resembling those of the diffusion-limited-aggregation (DLA) model [5] when a homopolymer solution is used. Recent experimental results [6] showed that the pattern-formation dynamics of non-Newtonian homopolymer solutions are much richer than that of simple Newtonian fluids with DLA-like clusters only one of a wide range of attainable patterns. Experiments using clay suspensions instead of polymer solutions have also shown a great richness of patterns [7]. In addition, a transition from a viscous-fingering pattern to a viscoelastic-fracturing pattern was observed in the clay system [8].

While it is well known that solutions of associating polymers can exhibit exotic viscoelastic properties, very little is known about their effects on nonequilibrium growth phenomena like pattern formation in a Hele-Shaw cell. In this paper we report the results of an experiment using associating polymers in a radial Hele-Shaw cell. Our associating polymer is composed of a long, water-soluble backbone terminated with water-insoluble end groups. Due to the hydrophobic end groups, associating polymers dissolving in water form a reversible network Our experiment compares the patterns formed in associating-polymer solutions with those formed in homopolymer solutions and permits us to comment on how the associating effects change the pattern-formation dynamics in Hele-Shaw experiments.

The model polymers we used in our experiment were provided by D. R. Bassett and R. D. Jenkins of Union Carbide [10] and have the following structure: R–O–(DI–PEO)$_Y$–DI–O–R, where R is a terminal group, DI isophorone diisocyanate, PEO is polyethylene oxide, and Y denotes the number of PEO units in the polymer backbone. The terminal group R can be either a hexadecyl end cap which is hydrophobic or a hydroxyl end cap (in which case the polymer is essentially a homopolymer). This allows us to compare the pattern-formation dynamics associated with the associating network and chain entanglement. For the hexadecyl–end-capped polymers, two molecular weights were used in the experiment: 17 400 and 50 700. For the hydroxyl–end-capped polymer, we used the molecular weight 100 400. The polymers were dissolved in distilled water. The concentrations of the hexadecyl–end-capped polymers were 2.5% and 2.0% by weight. The concentration of the hydroxyl–end-capped polymer was 20%. A 1.5% solution of polyethylene oxide of molecular weight 5×10^6 was also used. The experiment was performed in a radial Hele-Shaw cell consisting of two circular Pyrex glass plates of radius 20 cm and thickness 1.3 cm separated by a small gap (which was 0.4 mm for most flow realizations). Dyed water was injected from the center into the Hele-Shaw cell filled with a polymer solution. The injection rate was kept constant during each flow realization by a syringe pump. The two plates were clamped together firmly through two circular aluminum frames and the gap between the plates was set by precision wires. The deformation of the plate near its center during a flow run of high injection rate and high-viscosity solution was found to be much less than 3% of the gap thickness (using a displacement indicator). The intermolecular diffusion at the interface was negligible since the injection rate was sufficiently high that during the time of a flow realization the interface remained sharp. The evolution of patterns was recorded on a videotape using a CCD camera and an enhanced super-VHS recorder and later digitized for analysis using an eight-bit frame grabber with 640 × 480 pixels .

The rheological properties of these associating polymers have been studied by Jenkins [11]. One example of the peculiar features of solutions of these associating polymers is that their shear viscosity is very much higher at a given concentration than would be the case if the polymers were homopolymers of the same molecu-

lar weight. Another special feature of these associating polymers is that viscosity increases rapidly with decreasing chain length (i.e., as the relative importance of the associating end groups in these associating-polymer solutions increases). In addition to shear thinning (viscosity decreases with increasing shear rate), a phenomenon observed in most polymer solutions, shear thickening is present in a small range of shear rates for these associating polymers; but for the concentrations used in our experiment, the shear-thickening effect is negligible [11]. The polymer network relaxation time can be estimated from the inverse of the onset shear rate of the shear-thinning regime of the viscosity-shear-rate relation. For each solution used in this experiment, we measured the steady-shear viscosity at low shear rates (typically from 10^{-1} $\sec^{-1}$ up to the shear-thinning shear rate presented below) with a Brookfield Model DV-III programmable rheometer and found good agreement with the values reported by Jenkins, Silebi, and El-Aasser [11]. Similarly, whenever our rheometer could attain the shear-thinning shear rate for a given solution, our measurements agreed with the published values. Thus in the discussion and analysis below we have used the values reported by Jenkins, Silebi, and El-Aasser for the shear-thinning shear rate, the shear rate above which the solution's viscosity drops steeply, eventually attaining very low values.

For each solution, we performed many flow realizations at different injection rates from 0.2 to 77 ml/min. We found that the pattern was typically viscous fingering, characterized by a tip-splitting instability with splitting angles usually smaller than 45°, as long as the injection rate was sufficiently low. But for each solution of the associating polymer, there exists a threshold injection rate (which, as is discussed below, depends on the particular solution) beyond which the patterns resemble fracture patterns observed in brittle materials [12], characterized by a side-branching instability with branching angles close to 90°. The difference between a fingering pattern and a "fracture" pattern is very drastic and no ambiguity exists in distinguishing one from the other (this is normally true for individual patterns since branching angles alone allow the determination to be made, but the determination becomes especially easy when the video-recording is reviewed to allow side branching to be clearly distinguished from tip splitting). Exact measurement of the threshold injection rate was experimentally difficult because the system was so sensitive to initial conditions. There was always a narrow range of injection rates (but wide compared to the control achievable by our syringe pump) in which it was not possible to predict before a measurement whether the observed pattern would be viscous fingering or "fracture." However, the transition was sharper than our apparatus could measure in the sense that we never observed a pattern intermediate between fingering and fracture. We cannot comment on whether this apparent sharpness arises from the limits of our apparatus or from the nature of the transition itself (like a critical point in a second-order phase transition). Figure 1 shows four typical patterns of a 2.5% solution of hexadecyl–end-capped polymer of molecular weight 50 700 at several injection rates: (a) $Q = 1.0$ ml/min, (b) $Q = 1.0$ ml/min, (c) $Q = 5.0$ ml/min, and (d) $Q = 20$ ml/min. For this solution, the pattern was always of the viscous-fingering type if the injection rate was smaller than 0.6 ml/min and always of the fracturing type if the injection rate was greater than 1.0 ml/min. For injection rates between 0.6 and 1.0 ml/min, either a viscous-fingering pattern (observed three times), statistically very similar to the one shown in Fig. 1(a), or a fracturing pattern (observed five times), like the one shown in Fig. 1(b) with only two or three straight branches, is observed. Although we do not have enough flow runs in the crossover region to obtain a statistical probability of being in the fingering regime and fracturing regime, we did find that the occurrence of fracturing patterns was higher than that of fingering patterns (roughly two to one for many experimental configurations). We also found that, in the crossover region, the probability of observing a viscous-fingering pattern is higher when the injection rate is low and close to the viscous-fingering region and vice versa. The number of main branches of a fracturing pattern in the crossover region varies with a tendency to have fewer branches (can be as low as only one) when the injection rate is low. Leaving the crossover region in the fingering regime, the pattern morphology does not change significantly over the entire range of the injection rate tested in the experiment. Away from the threshold in the fracture regime, the pattern morphology changes dramatically with the injection rate (becoming more and more ramified and complicated with increasing injection rate) but never returns to viscous fingering.

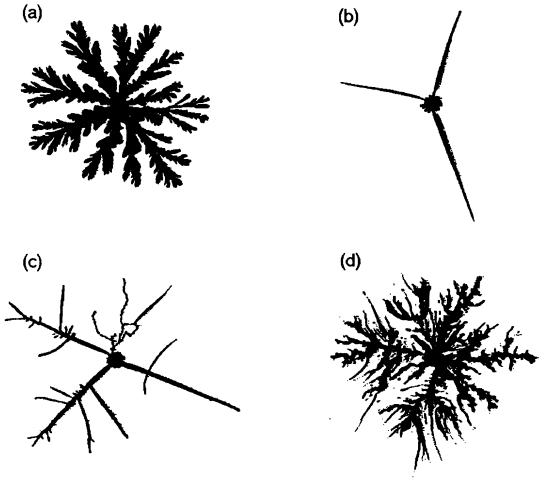

FIG. 1. Four typical patterns of a 2.5% solution of hexadecyl–end-capped polymer of molecular weight 50 700 at injection rates (a) $Q = 1.0$ ml/min, (b) $Q = 1.0$ ml/min, (c) $Q = 5.0$ ml/min, and (d) $Q = 20$ ml/min. The crossover from the viscous-fingering pattern to the fracturing pattern is seen in (a) and (b).

To our knowledge, the fingering-fracturing transition has not been observed in homopolymer solutions. We have performed experiments with a 20% solution of a hydroxyl–end-capped polymer of molecular weight 100 400 at injection rates up to 77 ml/min and we never observed fracture patterns. Due to the absence of the

associating network in this solution, the shear viscosity of this polymer solution at any given concentration is much lower than that of the associating-polymer solutions [11]. (We cannot specify this difference quantitatively in terms of the shear rate for the onset of shear thinning because the solution of the hydroxyl–end-capped polymer behaves like a Newtonian fluid over the entire range of shear rates achievable with our viscometer. However, at a low shear rate the 20% hydroxyl–end-capped polymer solution has viscosity 3000 cP while for the hexadecyl–end-capped polymers, the 2.5% molecular weight 50 700 solution has low-shear-rate viscosity 12 000 cP, the 2.5% molecular weight 17 400 solution has low-shear-rate viscosity 43 000 cP, and the 2.0% molecular weight 17 400 solution has low-shear-rate viscosity 32000 cP.) In order to further check whether fracture patterns occur in homopolymer solutions, we have performed several flow realizations at different injection rates from 0.2 to 77 ml/min using a strong viscoelastic solution of a high molecular weight (5 million) polyethylene oxide at concentration 1.5% by weight. This solution has viscosity 50 000 cP at low shear rate and a shear-thinning onset at shear rate below 0.1 sec^{-1}. Figure 2 shows four examples of patterns obtained at injection rates (a) 0.2 ml/min, (b) 1.0 ml/min, (c) 20 min ml/min, and (d) 77 ml/min. We can see clearly that patterns at all injection rates have the same viscous-fingering characteristics, changing only in the local finger profiles with injection rate. This observation suggests that the fingering-fracturing transition is either a direct result of associating-network effects or at least a manifestation of them. Further work is needed to understand why the highly entangled networks characteristic of concentrated homopolymer solutions do not lead to the fingering-fracturing transition.

It is interesting to note that the fingering-fracturing transition was also observed in a clay experiment by Lemaire *et al.* [8]. While it is generally true that a polymer solution is better understood rheologically than clay, the associating polymer is obviously very different from both of them. Although we do not understand the difference between the clay of Lemaire *et al.* and our associating polymer, we did notice a difference in the pattern morphologies: the transition is smooth and gradual for the clay experiment (see Fig. 1(b) of Ref. [8]) and the transition is abrupt for the associating polymer experiment.

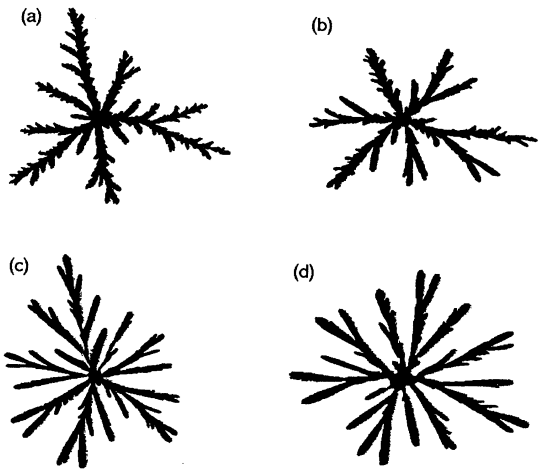

FIG. 2. Four typical patterns of a 1.5% homopolymer solution of molecular weight 5 000 000 at injection rates (a) $Q = 0.2$ ml/min, (b) $Q = 1.0$ ml/min, (c) $Q = 20$ ml/min, and (d) $Q = 77$ ml/min. The fingering-fracturing transition was not observed in the range of injection rates tested in the experiment.

Although Lemaire *et al.* [8] showed that the fingering-fracturing transition can be generated by plate deformation during the flow, we believe that this is probably not the case in our experiment for the following reasons: (1) The thickness of our plates (13 mm) is somewhat higher than their low-deformability cell (12 mm) and the size of our cell (20 cm in diameter) is much smaller than their cell (45 cm). Since the deformation is proportional to the size of the cell to the fourth power [8], the deformation of our cell should be much smaller than their low-deformability cell. (2) Most significantly, we have repeated our measurement for one of our solutions (2.0% molecular weight 17 400 hexadecyl–end-capped polymer) in a cell with thicker plates (22 mm) and find the fracture transition appearing in the same narrow range of injection rates. (3) We made a measurement (using a pressure transducer in the inlet tubing near the injection hole of the cell) of our injection pressure and found it to be at all times lower than 7×10^3 Pa for a flow run of high injection rate and a solution of high viscosity at low shear rate. This pressure must be measured rather than just estimated because the solution's shear viscosity is so strongly dependent on the local shear rate. The low value of measured pressure indicates unsurprisingly that the system is driven above its shear-thinning point. The measured pressure is too low to significantly bend a glass plate of this thickness and size [at 7×10^3 Pa pressure, the largest amplitude flexing of the plate should be 1.7% of the cell gap (0.4 mm) if the pressure difference is very pessimistically assumed to be applied across an area of radius 3 cm]. Actual measurement of the deformation showed that it was much smaller than 3% (which is the lower limit that our displacement indicator can detect) of the gap thickness for even the highest injection rate. As the discussion of Table I below indicates, the fracture transition has been observed for some solutions at injection rates $\sim$ 40 times lower than the value for which these conservative estimates of plate flexing are calculated, suggesting a plate flexing upper limit of $\sim$ 0.04%. (4) With the same deformability of our cell, the fingering-fracturing transition was not observed with the highly viscous homopolymer solutions at even the highest injection rates.

In addition to visually distinguishing the patterns, we have tried to formulate a quantitative classification of the patterns, as we did in our previous work on homopolymer solution patterns [6]. One very simple pattern measure which shows the fingering-fracuring transition involves calculating the mass fractal dimension for each of our patterns using the box-counting method [13]. In Fig. 3 we plot, in logarithmic scales, the area of invading water

TABLE I. Deborah-number scaling of the fingering-fracturing transition. MW denotes molecular weight and C denotes polymer concentration.

End group	MW (g/mol)	C (% wt)	$\dot{\gamma}_o$ (1/sec)	b (mm)	Expected Q_C (ml/min)	Observed Q_C (ml/min)
hexadecyl	50700	2.5	20[a]	0.4		0.6–1.0
hexadecyl	50700	2.5	20[a]	0.8	2.4–4.0	3.0–4.5
hexadecyl	17400	2.5	7[a]	0.4	0.2–0.4	0.3–0.5
hexadecyl	17400	2.0	10[a]	0.4	0.3–0.5	0.2–0.6
hydroxyl	100400	20	> 20	0.4	> 1.0	not observed[b]
hydroxyl	5000000	1.5	< 0.1	0.4	< 0.005	not observed[b]

[a]Extracted from Ref. [11].

[b]Up to the maximum accessible injection rate 77 ml/min.

enclosed by a circle centered at the orifice of the cell versus the radius of the circle for a few patterns obtained with the 2.5% solution of hexadecyl–end-capped polymer of molecular weight 50 700 at several different injection rates. The slope of the linear part of the data points of each injection rate gives the value of the fractal dimension of the corresponding pattern. A dramatic change of the fractal dimension near the fingering-fracturing transition is obvious. We can even more clearly see the abrupt change of the fractal dimension near the transition threshold when we plot the the fractal dimension as a function of the volumetric injection rate, as is shown in Fig. 4. Below the threshold, the patterns are of viscous-fingering type and the fractal dimensions are approximately 1.7. Above the threshold in the fracture regime, the fractal dimension suddenly drops to ~ 1.0 and then gradually recovers to 1.7 as the injection rate increases. Since fracturing is a quick process of releasing excessive stress built up in a material by external force which can not otherwise be released via other means, e.g., viscous dissipation, it is reasonable to expect the medium to respond to increasing injection rate with a rapid ramification of cracks which in turn results in an increase in the fractal dimension of the crack pattern. On the other hand, the fractal dimensions of the patterns shown in Fig. 2 for the homopolymer solution all fall onto the same value (approximately 1.5), even though the local structures of the patterns are slightly different from each other. This is seen in Fig. 5 where we plot the same variables as in Fig. 3 for the four homopolymer solution patterns. The above results suggest that the fractal-dimension analysis can be used as another quantitative characterization of the fingering-fracturing transition.

A useful method to characterize the flow of a viscoelastic material, like a polymer solution, is to define a Deborah number, the ratio of the polymer relaxation time τ_r to the characteristic time of the fluid flow τ_f [14]. The characteristic time for the Hele-Shaw flow is expected to be proportional to rb^2/Q, where b is the gap of the Hele-

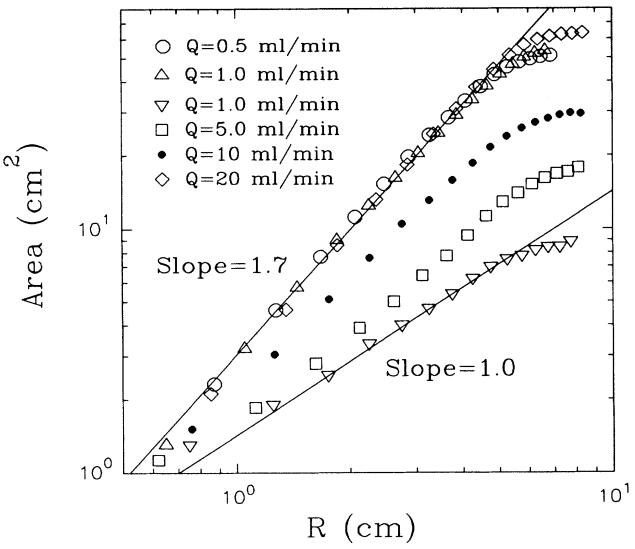

FIG. 3. Area of the invading water enclosed by a circle centered at the orifice of the Hele-Shaw cell vs the radius of the circle R for a few patterns obtained with a 2.5% solution of a hexadecyl–end-capped polymer of molecular weight 50 700 at different injection rates as shown in the legend. The fractal dimension of a pattern is calculated from the slope of the linear part of the data points. Two straight lines of slopes 1.0 and 1.7 are also shown in the figure for reference.

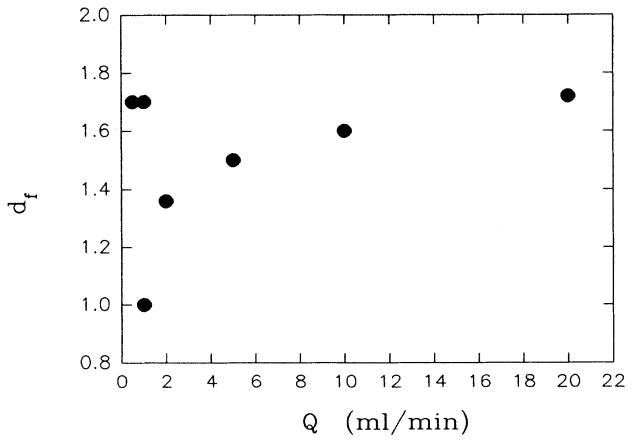

FIG. 4. The mass fractal dimension d_f vs the injection rate Q for the patterns obtained with a 2.5% solution of hexadecyl–end-capped polymer of molecular weight 50 700. The fingering-fracturing transition is associated with an abrupt decrease in the pattern's fractal dimension.

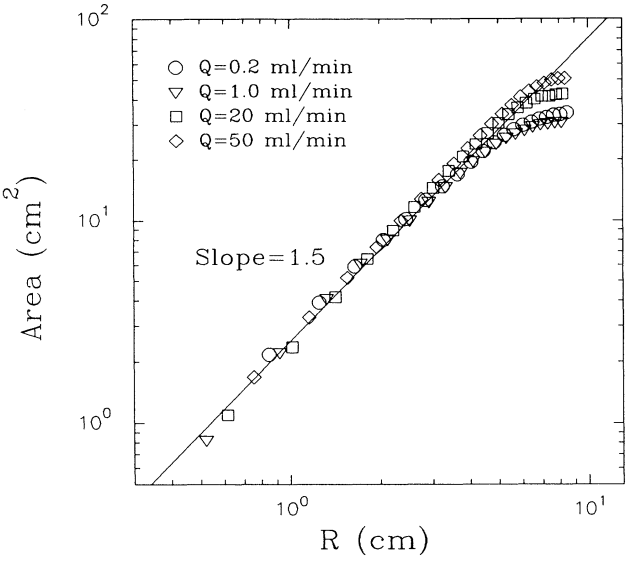

FIG. 5. Area of the invading water enclosed by a circle centered at the orifice of the Hele-Shaw cell vs the radius of the circle R for the patterns obtained with a homopolymer solution (1.5% PEO of molecular weight 5 000 000) at different injection rates as shown in the legend. A straight line of slope 1.5 is also shown in the figure for reference.

Shaw cell and r is a length scale, e.g., the radius of the Hele-Shaw cell. So the Deborah number scales as

$$\mathrm{De} \equiv \frac{\tau_r}{\tau_f} \sim \frac{Q\tau_r}{b^2} = \frac{Q}{b^2\dot{\gamma}_o} . \quad (1)$$

Here in the last equation we have used the inverse of the onset shear rate ($\dot{\gamma}_o$) of the shear-thinning regime as our approximation for the polymer relaxation time [15]. We could change the Deborah number by changing the polymer molecular weight, the polymer concentration, the Hele-Shaw cell gap, and the injection rate. Since the fingering-fracturing transition is a crossover of natures from viscous fluid to elastic solid, one might expect the transition to happen at the same Deborah number for different flow configurations. We have repeated the experiment both by doubling the Hele-Shaw cell gap b and by varying $\dot{\gamma}_o$ via changing the solution. We find that we can roughly predict the crossover injection rate by assuming that the transition always occurs at the same Deborah number. Our results are listed in Table I: the onset shear rates for the shear-thinning regime of the associating-polymer solutions were extracted from Ref. [11]. The expected threshold injection rates are based on the Deborah-number scaling of Eq. (1), using the observed value of the 2.5% solution of the hexadecyl–end-capped polymer of molecular weight 50 700 at $b = 0.4$ mm (first row). The observed threshold injection rates for the fingering-fracturing transition in double gap (second row), low molecular weight 17 400 (third row), and different concentration (fourth row) flows are in agreement with the expected values, indicating that the fingering-fracturing transition in the associating-polymer solution does follow the Deborah-number scaling.

The last two rows of the table give estimates of the injection rates to achieve a similarly defined transition Deborah number for the homopolymer flows (hydroxyl–end-capped) discussed above. These rows indicate that our observations took these systems far above the Deborah number which would be required for the transition if the entanglement relaxations in these solutions were dynamically equivalent to the relaxation of the associating network. Polymer solutions can show a variety of relaxation times [16], so it is perhaps not surprising that using the inverse of the shear-thinning shear rate alone to describe the polymer solution's relaxation works for only a limited class of samples. Further work is needed to determine which property (or properties) contributes to making the fracture of the associating polymer solution depend so closely on the shear-thinning shear rate when this is not the case for the homopolymer.

In summary, we have performed Hele-Shaw experiments using polymer solutions and demonstrated a fingering-fracturing transition which is present when the polymer forms an associating network in solution and is absent if the polymer dynamics was mainly controlled by chain entanglement. This transition is very abrupt (although sensitivity to initial conditions makes it difficult to determine the exact threshold) as the injection rate is increased and it is associated with an abrupt decrease in the pattern's mass fractal dimension. As the injection rate is further increased above the threshold region, the patterns retain their fracturelike character but become more and more ramified and complicated with the fractal dimension gradually recovering to the one observed below the crossover.

We thank D. R. Bassett and R. D. Jenkins of the Union Carbide Laboratories for providing the model associating polymers and for helpful discussions. This work was supported by the National Science Foundation under Grant No. DMR-9001518.

[1] D. Bensimon, L. P. Kadanoff, S. Liang, B. I. Shraiman, and C. Tang, Rev. Mod. Phys. **58**, 977 (1986).
[2] G. M. Homsy, Annu. Rev. Fluid Mech. **19**, 271 (1987).
[3] J. Nittman, G. Daccord, and H. E. Stanley, Nature (London) **314**, 141 (1985).
[4] G. Daccord, J. Nittman, and H. E. Stanley, Phys. Rev. Lett. **56**, 336 (1986).
[5] T. A. Witten and L. M. Sander, Phys. Rev. Lett. **47**, 1400 (1981).
[6] H. Zhao and J. V. Maher, Phys. Rev. A **45**, R8328 (1992).
[7] H. van Damme, C. Laroche, and P. Levitz, J. Phys. (Paris) **48**, 1221 (1987).
[8] E. Lemaire, P. Levitz, G. Daccord, and H. van Damme, Phys. Rev. Lett. **67**, 2009 (1991).
[9] P. G. de Gennes, *Scaling Concepts in Polymer Physics* (Cornell University, Ithaca, 1979).

[10] Union Carbide Chemicals and Plastics Company Inc., P.O. Box 8361, South Charleston, WV 25303.
[11] R. D. Jenkins, C. A. Silebi, and M. S. El-Aasser, in *Polymers as Rheology Modifiers*, edited by Donald N. Schulz and J. Edward Glass, ACS Symposium Series No. 462, p. 222 (American Chemical Society, Washington, DC, 1991); R. D. Jenkins, Ph. D. thesis, Lehigh University, 1990 (unpublished).
[12] *Statistical Models for the Fracture of Disorderd Media*, edited by H. J. Herrmann and S. Roux (North-Holland, Amsterdam, 1990).
[13] J. Feder, *Fractals* (Plenum, New York, 1988).
[14] M. Reiner, Phys. Today **17** (1), 62 (1964).
[15] W. W. Graessley, in *Physical Properties of Polymers*, edited by J. E. Mark *et al.* (American Chemical Society, Washington, DC, 1984).
[16] M. Doi and S. F. Edwards, *The Theory of Polymer Dynamics* (Oxford, New York, 1986).